1

BASIC CONCEPTS

1.1 INTRODUCTION

Concrete is strong in compression, but weak in tension: its tensile strength varies from 8 to 14 percent of its compressive strength. Due to such a low tensile capacity, flexural cracks develop at early stages of loading. In order to reduce or prevent such cracks from developing, a concentric or eccentric force is imposed in the longitudinal direction of the structural element. This force prevents the cracks from developing by eliminating or considerably reducing the tensile stresses at the critical midspan and support sections at service load, thereby raising the bending, shear, and torsional capacities of the sections. The sections are then able to behave elastically, and almost the full capacity of the concrete in compression can be efficiently utilized across the entire depth of the concrete sections when all loads act on the structure.

Such an imposed longitudinal force is called a *prestressing force,* i.e., a compressive force that prestresses the sections along the span of the structural element prior to the application of the transverse gravity dead and live loads or transient horizontal live loads. The type of prestressing force involved, together with its magnitude, are determined mainly on the basis of the type of system to be constructed and the span length and slenderness desired. Since the prestressing force is applied longitudinally along or parallel to

The Diamond Baseball Stadium, Richmond, Virginia. Situ cast and precast post-tensioned prestressed structure. (*Courtesy,* Prestressed Concrete Institute.)

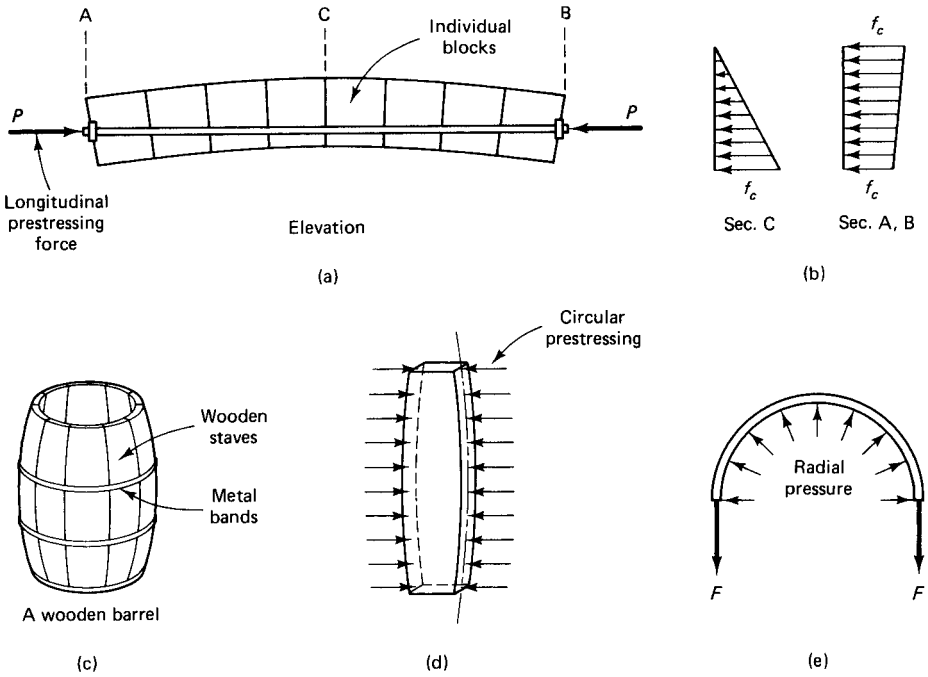

Figure 1.1 Prestressing principle in linear and circular prestressing. (a) Linear prestressing of a series of blocks to form a beam. (b) Compressive stress on midspan section C and end section A or B. (c) Circular prestressing of a wooden barrel by tensioning the metal bands. (d) Circular hoop prestress on one wooden stave. (e) Tensile force F on half of metal band due to internal pressure, to be balanced by circular hoop prestress.

the axis of the member, the prestressing principle involved is commonly known as *linear* prestressing.

Circular prestressing, used in liquid containment tanks, pipes, and pressure reactor vessels, essentially follows the same basic principles as does linear prestressing. The circumferential hoop, or "hugging" stress on the cylindrical or spherical structure, neutralizes the tensile stresses at the outer fibers of the curvilinear surface caused by the internal contained pressure.

Figure 1.1 illustrates, in a basic fashion, the prestressing action in both types of structural systems and the resulting stress response. In (a), the individual concrete blocks act together as a beam due to the large compressive prestressing force *P.* Although it might appear that the blocks will slip and vertically simulate shear slip failure, in fact they will not because of the longitudinal force *P.* Similarly, the wooden staves in (c) might appear to be capable of separating as a result of the high internal radial pressure exerted on them. But again, because of the compressive prestress imposed by the metal bands as a form of circular prestressing, they will remain in place.

1.1.1 Comparison with Reinforced Concrete

From the preceding discussion, it is plain that permanent stresses in the prestressed structural member are created before the full dead and live loads are applied, in order to eliminate or considerably reduce the net tensile stresses caused by these loads. With reinforced concrete, it is assumed that the tensile strength of the concrete is negligible

Photo 1.1 Bay Area Rapid Transit (BART), San Francisco and Oakland, California. Guideways consist of prestressed precast simple-span box girders 70 ft long and 11 ft wide. (*Courtesy,* Bay Area Rapid Transit District, Oakland, California.)

and disregarded. This is because the tensile forces resulting from the bending moments are resisted by the bond created in the reinforcement process. Cracking and deflection are therefore essentially irrecoverable in reinforced concrete once the member has reached its limit state at service load.

The reinforcement in the reinforced concrete member does not exert any force of its own on the member, contrary to the action of prestressing steel. The steel required to produce the prestressing force in the prestressed member actively preloads the member, permitting a relatively high controlled recovery of cracking and deflection. Once the flex-

Photo 1.2 Chaco-Corrientes Bridge, Argentina. The longest precast prestressed concrete cable-stayed box girder bridge in South America. (*Courtesy,* Ammann & Whitney.)

Photo 1.3 Park Towers, Tulsa, Oklahoma. (*Courtesy,* Prestressed Concrete Institute.)

ural tensile strength of the concrete is exceeded, the prestressed member starts to act like a reinforced concrete element.

By controlling the amount of prestress, a structural system can be made either flexible or rigid without influencing its strength. In reinforced concrete, such a flexibility in behavior is considerably more difficult to achieve if considerations of economy are to be observed in the design. Flexible structures such as fender piles in wharves have to be highly energy absorbent, and prestressed concrete can provide the required resiliency. Structures designed to withstand heavy vibrations, such as machine foundations, can easily be made rigid through the contribution of the prestressing force to the reduction of their otherwise flexible deformation behavior.

1.1.2 Economics of Prestressed Concrete

Prestressed members are shallower in depth than their reinforced concrete counterparts for the same span and loading conditions. In general, the depth of a prestressed concrete member is usually about 65 to 80 percent of the depth of the equivalent reinforced concrete member. Hence, the prestressed member requires less concrete, and about 20 to 35 percent of the amount of reinforcement. Unfortunately, this saving in material weight is balanced by the higher cost of the higher quality materials needed in prestressing. Also, regardless of the system used, prestressing operations themselves result in an added cost: Formwork is more complex, since the geometry of prestressed sections is usually composed of flanged sections with thin webs.

In spite of these additional costs, if a large enough number of precast units are manufactured, the difference between at least the initial costs of prestressed and reinforced concrete systems is usually not very large. And the indirect long-term savings are quite substantial, because less maintenance is needed, a longer working life is possible due to

better quality control of the concrete, and lighter foundations are achieved due to the smaller cumulative weight of the superstructure.

Once the beam span of reinforced concrete exceeds 70 to 90 feet, the dead weight of the beam becomes excessive, resulting in heavier members and, consequently, greater long-term deflection and cracking. Thus, for larger spans, prestressed concrete becomes mandatory since arches are expensive to construct and do not perform as well due to the severe long-term shrinkage and creep they undergo. Very large spans such as segmental bridges or cable-stayed bridges can *only* be constructed through the use of prestressing.

1.2 HISTORICAL DEVELOPMENT OF PRESTRESSING

Prestressed concrete is not a new concept, dating back to 1872, when P. H. Jackson, an engineer from California, patented a prestressing system that used a tie rod to construct beams or arches from individual blocks. [See Figure 1.1(a).] In 1888, C. W. Doehring of Germany obtained a patent for prestressing slabs with metal wires. But these early attempts at prestressing were not really successful because of the loss of the prestress with time. J. Lund of Norway and G. R. Steiner of the United States tried early in the twentieth century to solve this problem, but to no avail.

After a long lapse of time during which little progress was made because of the unavailability of high-strength steel to overcome prestress losses, R. E. Dill of Alexandria, Nebraska, recognized the effect of the shrinkage and creep (transverse material flow) of concrete on the loss of prestress. He subsequently developed the idea that successive post-tensioning of *unbonded* rods would compensate for the time-dependent loss of stress in the rods due to the decrease in the length of the member because of creep and shrinkage. In the early 1920s, W. H. Hewett of Minneapolis developed the principles of circular prestressing. He hoop-stressed horizontal reinforcement around walls of concrete tanks through the use of turnbuckles to prevent cracking due to internal liquid pres-

Photo 1.4 Wiscasset Bridge, Maine. (*Courtesy,* Post-Tensioning Institute.)

Photo 1.5 Executive Center, Honolulu, Hawaii. (*Courtesy,* Post-Tensioning Institute.)

sure, thereby achieving watertighteness. Thereafter, prestressing of tanks and pipes developed at an accelerated pace in the United States, with thousands of tanks of water, liquid, and gas storage built and much mileage of prestressed pressure pipe laid in the two to three decades that followed.

Linear prestressing continued to develop in Europe and in France, in particular through the ingenuity of Eugene Freyssinet, who proposed in 1926 through 1928 methods to overcome prestress losses through the use of high-strength and high-ductility steels. In 1940, he introduced the now well-known and well-accepted Freyssinet system comprising the conical wedge anchor for 12-wire tendons.

During World War II and thereafter, it became necessary to reconstruct in a prompt manner many of the main bridges that were destroyed by war activities. G. Magnel of Ghent, Belgium, and Y. Guyon of Paris extensively developed and used the concept of prestressing for the design and construction of numerous bridges in western and central Europe. The Magnel system also used wedges to anchor the prestressing wires. They differed from the original Freyssinet wedges in that they were flat in shape, accommodating the prestressing of two wires at a time.

P. W. Abeles of England introduced and developed the concept of partial prestressing between the 1930s and 1960s. F. Leonhardt of Germany, V. Mikhailov of Russia, and T. Y. Lin of the United States also contributed a great deal to the art and science of the design of prestressed concrete. Lin's load-balancing method deserves particular mention in this regard, as it considerably simplified the design process, particularly in continuous structures. These twentieth-century developments have led to the extensive use of prestressing throughout the world, and in the United States in particular.

Photo 1.6 Stratford "B" Condeep offshore oil drilling platform, Norway. (*Courtesy,* the late Ben C. Gerwick.)

Today, prestressed concrete is used in buildings, underground structures, TV towers, floating storage and offshore structures, power stations, nuclear reactor vessels, and numerous types of bridge systems including segmental and cable-stayed bridges. Note the variety of prestressed structures in the photos throughout the book; they demonstrate the versatility of the prestressing concept and its all-encompassing applications. The success in the development and construction of all these landmark structures has been due in no small measure to the advances in the technology of materials, particularly prestressing steel, and the accumulated knowledge in estimating the short- and long-term losses in the prestressing forces.

1.3 BASIC CONCEPTS OF PRESTRESSING

1.3.1 Introduction

The prestressing force P that satisfies the particular conditions of geometry and loading of a given element (see Figure 1.2) is determined from the principles of mechanics and of stress-strain relationships. Sometimes simplification is necessary, as when a prestressed beam is assumed to be homogeneous and elastic.

Consider, then, a simply supported rectangular beam subjected to a *concentric* prestressing force P as shown in Figure 1.2(a). The compressive stress on the beam cross section is uniform and has an intensity

Photo 1.7 Sunshine Skyway Bridge, Tampa Bay, Florida. Designed by Figg and Muller Engineers, Inc., the bridge has a 1,200-ft cable-stayed main span with a single pylon, 175-ft vertical clearance, and total length of 21,878 ft. It has twin 40-ft roadways and has 135-ft spans in precast segmental sections and high approaches to elevation + 130 ft. (*Courtesy,* Figg and Muller Engineers, Inc., now FIGG Engineers)

$$f = -\frac{P}{A_c} \tag{1.1}$$

where $A_c = bh$ is the cross-sectional area of a beam section of width b and total depth h. A *minus* sign is used for compression and a *plus* sign for tension throughout the text. Also, bending moments are drawn on the tensile side of the member.

If external transverse loads are applied to the beam, causing a maximum moment M at midspan, the resulting stress becomes

$$f^t = -\frac{P}{A} - \frac{Mc}{I_g} \tag{1.2a}$$

and

$$f_b = -\frac{P}{A} + \frac{Mc}{I_g} \tag{1.2b}$$

where f^t = stress at the top fibers
f_b = stress at the bottom fibers
$c = \frac{1}{2}h$ for the rectangular section
I_g = gross moment of inertia of the section ($bh^3/12$ in this case)

Equation 1.2b indicates that the presence of prestressing-compressive stress $-P/A$ is reducing the tensile flexural stress Mc/I to the extent intended in the design, either elimi-

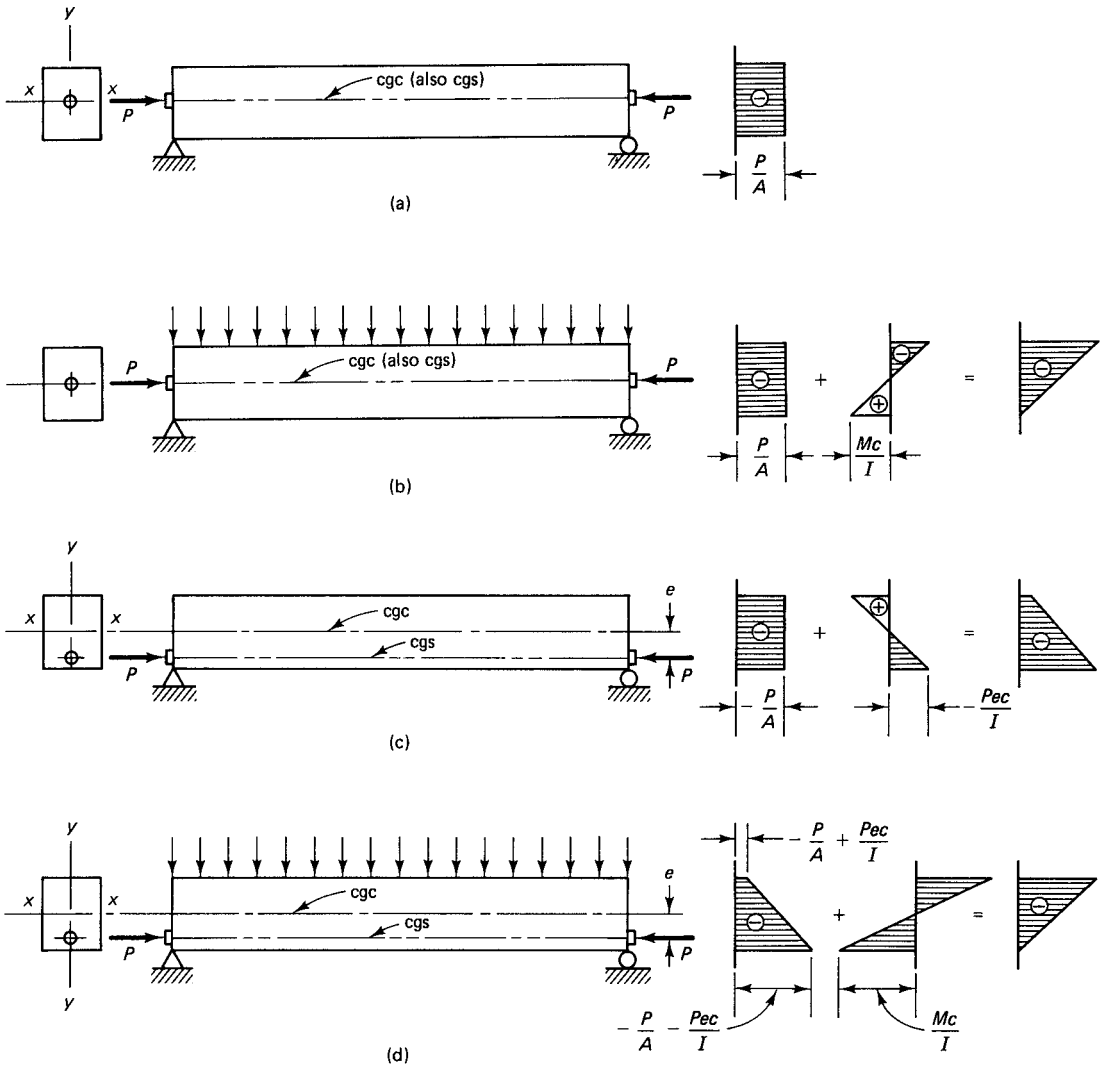

Figure 1.2 Concrete fiber stress distribution in a rectangular beam with straight tendon. (a) Concentric tendon, prestress only. (b) Concentric tendon, self-weight added. (c) Eccentric tendon, prestress only. (d) Eccentric tendon, self-weight added.

nating tension totally (even inducing compression), or permitting a level of tensile stress within allowable code limits. The section is then considered uncracked and behaves elastically: the concrete's inability to withstand tensile stresses is effectively compensated for by the compressive force of the prestressing tendon.

The compressive stresses in Equation 1.2a at the top fibers of the beam due to prestressing are compounded by the application of the loading stress $-Mc/I$, as seen in Figure 1.2(b). Hence, the compressive stress capacity of the beam to take a substantial external load is reduced by the *concentric* prestressing force. In order to avoid this limitation, the prestressing tendon is placed *eccentrically* below the neutral axis at midspan, to induce tensile stresses at the top fibers due to prestressing. [See Figure 1.2(c), (d).] If the tendon is placed at eccentricity e from the center of gravity of the concrete, termed the *cgc line,* it creates a moment Pe, and the ensuing stresses at midspan become

Photo 1.8 The new I-35W bridge, Minneapolis, Minnesota. Designed by FIGG, the 10-lane interstate bridge has a 504′ precast, prestressed concrete span over the Mississippi River, with 75′ vertical clearance. The span's 120 precast concrete segments, each 45′ wide, up to 25′ deep and weighing 200 tons, achieved an average concrete strength of 7600 psi. These segments for the main span were assembled in one directional cantilever from the main piers in just 47 days. The bridge has 50,000 cubic yards of concrete and nearly 3 million pounds of post-tensioning steel that runs the length of the twin 1,214′ bridges. This new interstate bridge was designed and built in 11 months, opening on September 18, 2008. (Courtesy of FIGG, the bridge designer)

$$f^t = -\frac{P}{A_c} + \frac{Pec}{I_g} - \frac{Mc}{I_g} \tag{1.3a}$$

$$f_b = -\frac{P}{A_c} - \frac{Pec}{I_g} + \frac{Mc}{I_g} \tag{1.3b}$$

Since the support section of a simply supported beam carries no moment from the external transverse load, high tensile fiber stresses at the top fibers are caused by the eccentric prestressing force. To limit such stresses, the eccentricity of the prestressing tendon profile, the *cgs line,* is made less at the support section than at the midspan section, or eliminated altogether, or else a negative eccentricity above the cgc line is used.

1.3.2 Basic Concept Method

In the basic concept method of designing prestressed concrete elements, the concrete fiber stresses are *directly* computed from the external forces applied to the concrete by longitudinal prestressing and the external transverse load. Equations 1.3a and b can be modified and simplified for use in calculating stresses at the initial prestressing stage and at service load levels. If P_i is the initial prestressing force before stress losses, and P_e is the effective prestressing force after losses, then

$$\gamma = \frac{P_e}{P_i} \tag{1.3c}$$

can be defined as the residual prestress factor. Substituting r^2 for I_g/A_c in Equations 1.3, where r is the radius of gyration of the gross section, the expressions for stress can be rewritten as follows:

(a) Prestressing Force Only

$$f^t = -\frac{P_i}{A_c}\left(1 - \frac{ec_t}{r^2}\right) \tag{1.4a}$$

Photo 1.9 Tianjin Yong-He cable-stayed prestressed concrete bridge, Tianjin, China, the largest span bridge in Asia, with a total length of 1,673 ft and a suspended length of 1,535 ft, was completed in 1988. (*Credits* Owner: Tianjin Municipal Engineering Bureau. General contractor: Major Bridge Engineering Bureau of Ministry of Railways of China. Engineer for project design and construction control guidance: Tianjin Municipal Engineering Survey and Design Institute, Chief Bridge Engineer, Bang-yan Yu.)

$$f_b = -\frac{P_i}{A_c}\left(1 + \frac{ec_b}{r^2}\right) \tag{1.4b}$$

where c_t and c_b are the distances from the center of gravity of the section (the cgc line) to the extreme top and bottom fibers, respectively.

(b) Prestressing Plus Self-weight

If the beam self-weight causes a moment M_D at the section under consideration, Equations 1.4a and b, respectively, become

$$f^t = -\frac{P_i}{A_c}\left(1 - \frac{ec_t}{r^2}\right) - \frac{M_D}{S^t} \tag{1.5a}$$

and

$$f_b = -\frac{P_i}{A_c}\left(1 + \frac{ec_b}{r^2}\right) + \frac{M_D}{S_b} \tag{1.5b}$$

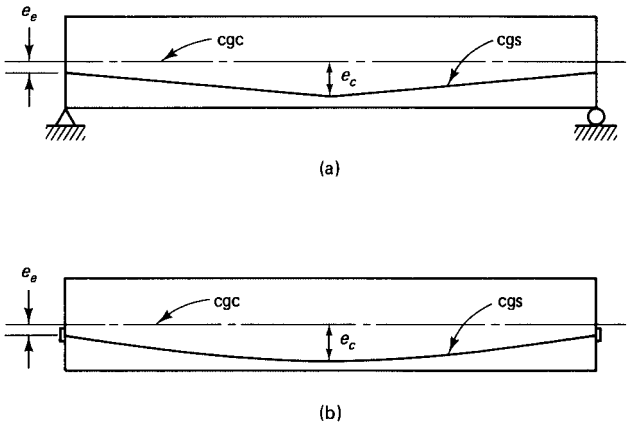

Figure 1.3 Prestressing tendon profile. (a) Harped tendon. (b) Draped tendon.

where S^t and S_b are the moduli of the sections for the top and bottom fibers, respectively.

The change in eccentricity from the midspan to the support section is obtained by raising the prestressing tendon either abruptly from the midspan to the support, a process called harping, or gradually in a parabolic form, a process called draping. Figure 1.3(a) shows a harped profile usually used for pretensioned beams and for concentrated transverse loads. Figure 1.3(b) shows a draped tendon usually used in post-tensioning.

Subsequent to erection and installation of the floor or deck, live loads act on the structure, causing a superimposed moment M_s. The full intensity of such loads normally occurs after the building is completed and some time-dependent losses in prestress have already taken place. Hence, the prestressing force used in the stress equations would have to be the effective prestressing force P_e. If the total moment due to gravity loads is M_T, then

$$M_T = M_D + M_{SD} + M_L \tag{1.6}$$

where M_D = moment due to self-weight
M_{SD} = moment due to superimposed dead load, such as flooring
M_L = moment due to live load, including impact and seismic loads if any

Equations 1.5 then become

$$f^t = -\frac{P_e}{A_c}\left(1 - \frac{ec_t}{r^2}\right) - \frac{M_T}{S^t} \tag{1.7a}$$

$$f_b = -\frac{P_e}{A_c}\left(1 + \frac{ec_b}{r^2}\right) + \frac{M_T}{S_b} \tag{1.7b}$$

Some typical elastic concrete stress distributions at the critical section of a prestressed flanged section are shown in Figure 1.4. The tensile stress in the concrete in part (c) permitted at the extreme fibers of the section cannot exceed the maximum permissible in the code, e.g., $f_t = 6\sqrt{f'_c}$ at midspan in the ACI code. If it is exceeded, bonded nonprestressed reinforcement proportioned to resist the total tensile force has to be provided to control cracking at service loads.

1.3.3 C-Line Method

In this line-of-pressure or thrust concept, the beam is analyzed as if it were a plain concrete elastic beam using the basic principles of statics. The prestressing force is considered an ex-

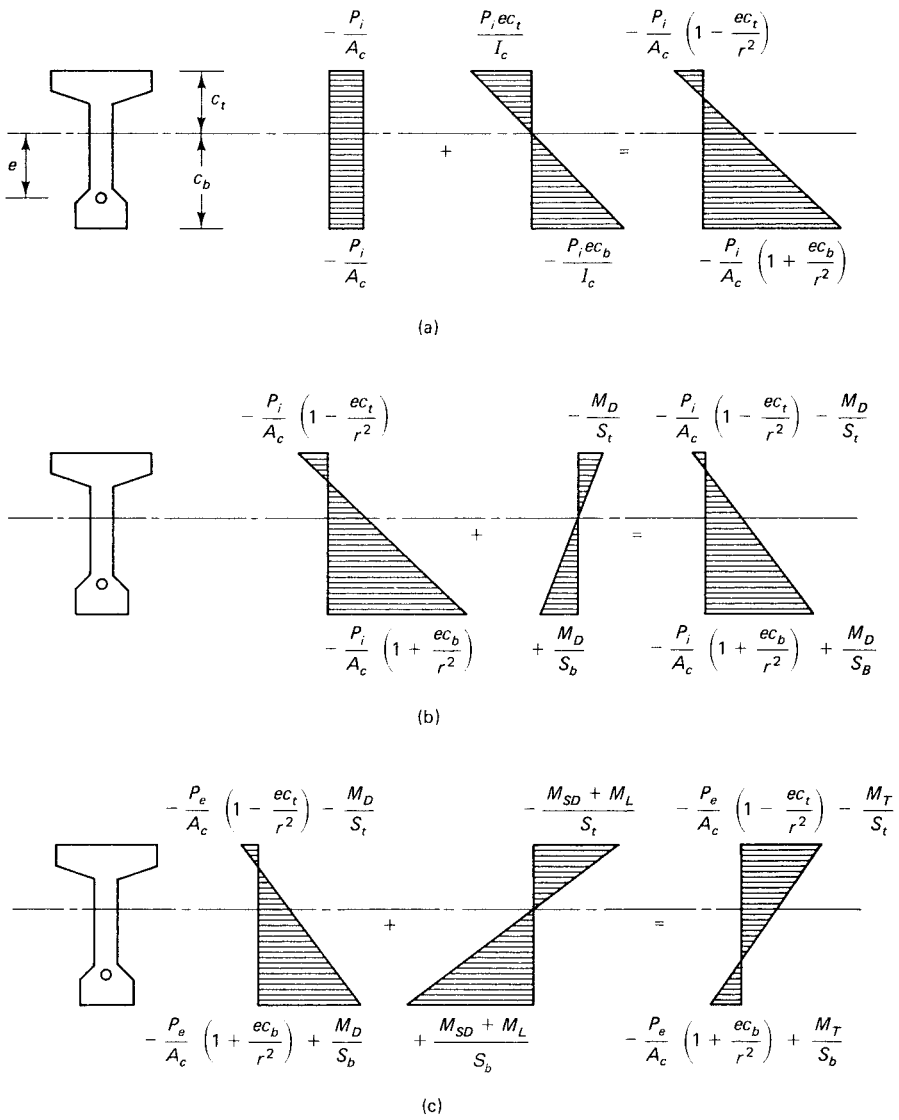

Figure 1.4 Elastic fiber stresses due to the various loads in a prestressed beam. (a) Initial prestress before losses. (b) Addition of self-weight. (c) Service load at effective prestress.

ternal compressive force, with a constant tensile force T in the tendon throughout the span. In this manner, the effects of external gravity loads are disregarded. Equilibrium equations $\Sigma H = 0$ and $\Sigma M = 0$ are applied to maintain equilibrium in the section.

Figure 1.5 shows the relative line of action of the compressive force C and the tensile force T in a reinforced concrete beam as compared to that in a prestressed concrete beam. It is plain that in a reinforced concrete beam, T can have a finite value only when transverse and other external loads act. The moment arm a remains basically constant throughout the elastic loading history of the reinforced concrete beam while it changes from a value $a = 0$ at prestressing to a maximum at full superimposed load.

Taking a free-body diagram of a segment of a beam as in Figure 1.6, it is evident that the C-line, or center-of-pressure line, is at a varying distance a from the T-line. The moment is given by

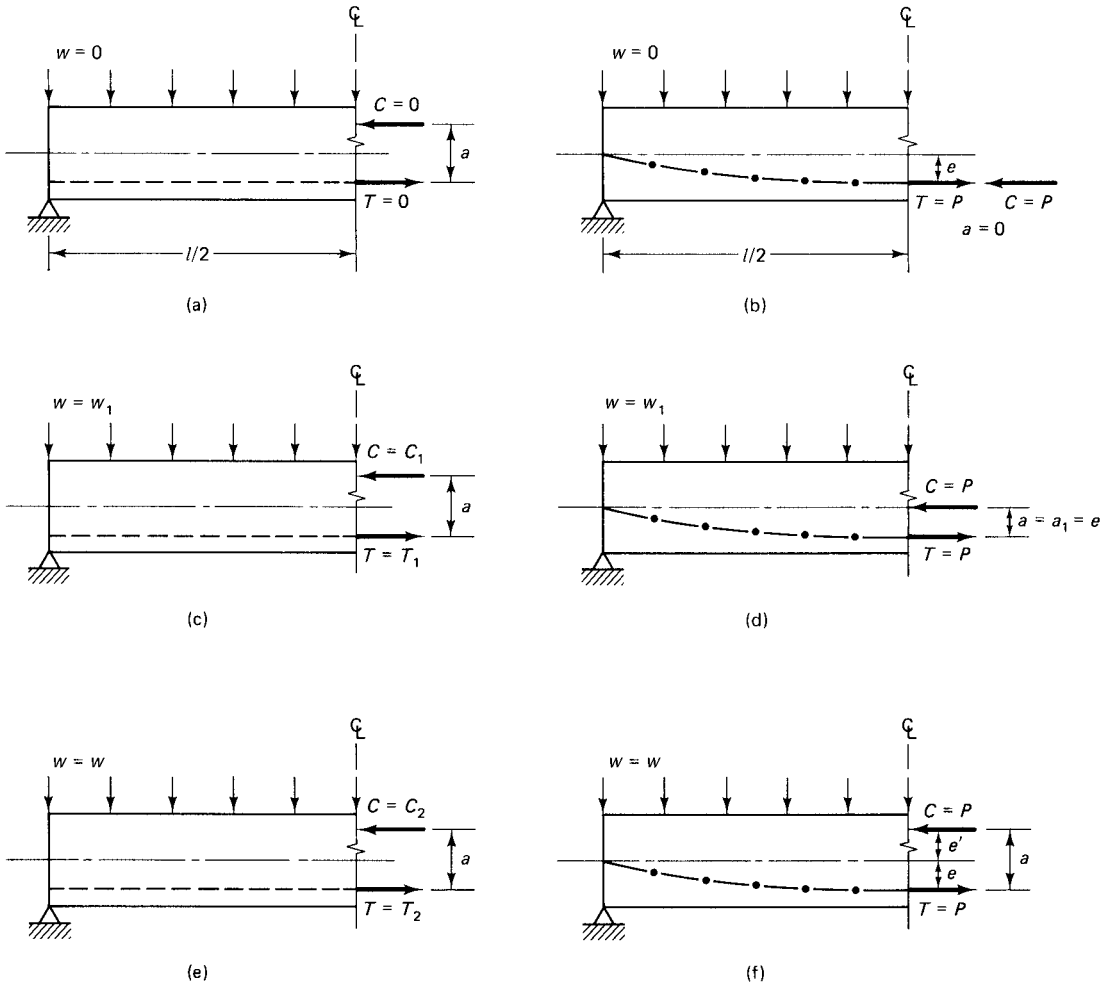

Figure 1.5 Comparative free-body diagrams of a reinforced concrete (R.C.) beam and a prestressed concrete (P.C.) beam. (a) R.C. beam with no load. (b) P.C. beam with no load. (c) R.C. beam with load w_1. (d) P.C. beam with load w_1. (e) R.C. beam with typical load w. (f) P.C. beam with typical load w.

$$M = Ca = Ta \tag{1.8}$$

and the eccentricity e is known or predetermined, so that in Figure 1.6,

$$e' = a - e \tag{1.9a}$$

Since $C = T$, $a = M/T$, giving

$$e' = \frac{M}{T} - e \tag{1.9b}$$

From the figure,

$$f^t = -\frac{C}{A_c} - \frac{Ce'c_t}{I_c} \tag{1.10a}$$

$$f_b = -\frac{C}{A_c} + \frac{Ce'c_b}{I_c} \tag{1.10b}$$

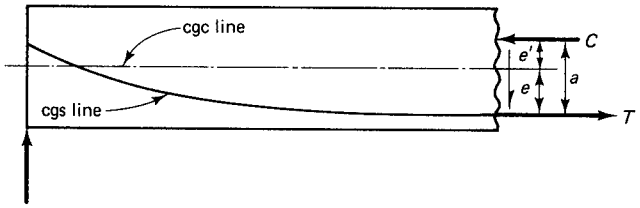

Figure 1.6 Free-body diagram for the C-line (center of pressure).

But in the tendon the force T equals the prestressing force P_e; so

$$f^t = -\frac{P_e}{A_c} - \frac{P_e e' c_t}{I_c} \tag{1.11a}$$

$$f_b = -\frac{P_e}{A_c} + \frac{P_e e' c_b}{I_c} \tag{1.11b}$$

Since $I_c = A_c r^2$, Equations 1.11a and b can be rewritten as

$$f^t = -\frac{P_e}{A_c}\left(1 + \frac{e' c_t}{r^2}\right) \tag{1.12a}$$

$$f_b = -\frac{P_e}{A_c}\left(1 - \frac{e' c_b}{r^2}\right) \tag{1.12b}$$

Equations 1.12a and b and Equations 1.7a and b should yield identical values for the fiber stresses.

1.3.4 Load-Balancing Method

A third useful approach in the design (analysis) of continuous prestressed beams is the load-balancing method developed by Lin and mentioned earlier. This technique is based on utilizing the vertical force of the draped or harped prestressing tendon to counteract or balance the imposed gravity loading to which a beam is subjected. Hence, it is applicable to nonstraight prestressing tendons.

Photo 1.10 East Huntington Bridge over Ohio River. A segmentally assembled precast prestressed concrete cable-stayed bridge spanning 200–900–608 ft. (*Courtesy,* Arvid Grant and Associates, Inc.)

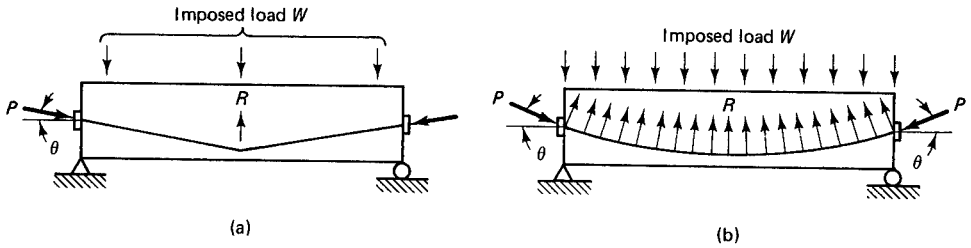

Figure 1.7 Load-balancing forces. (a) Harped tendon. (b) Draped tendon.

Figure 1.7 demonstrates the balancing forces for both harped- and draped-tendon prestressed beams. The load balancing reaction R is equal to the vertical component of the prestressing force P. The horizontal component of P, as an approximation in long-span beams, is taken to be equal to the full force P in computing the concrete fiber stresses *at midspan* of the simply supported beam. At other sections, the actual horizontal component of P is used.

1.3.4.1 Load-Balancing Distributed Loads and Parabolic Tendon Profile. Consider a parabolic tendon as shown in Figure 1.8. Let the parabolic function

$$Ax^2 + Bx + C = y \tag{1.13}$$

represent the tendon drape; the force T denotes the pull to which the tendon is subjected. Then for $x = 0$, we have

$$y = 0 \qquad C = 0$$

$$\frac{dy}{dx} = 0 \qquad B = 0$$

and for $x = l/2$,

$$y = a \qquad A = \frac{4a}{l^2}$$

But from calculus, the load intensity is

$$q = T\frac{\partial^2 y}{\partial x^2} \tag{1.14}$$

Finding $\partial^2 y/\partial x^2$ in Equation 1.13 and substituting into Equation 1.14 yields

$$q = T\frac{4a}{l^2} \times 2 = \frac{8Ta}{l^2} \tag{1.15a}$$

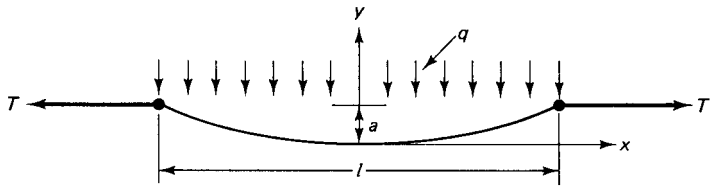

Figure 1.8 Sketched tendon subjected to transverse load intensity q.

or

$$T = \frac{ql^2}{8a} \tag{1.15b}$$

$$Ta = \frac{ql^2}{8} \tag{1.15c}$$

Hence, if the tendon has a parabolic profile in the prestressed beam and the prestressing force is denoted by P, the balanced-load intensity, from Equation 1.15a, is

$$w_b = \frac{8Pa}{l^2} \tag{1.16}$$

Figure 1.9 gives a free-body diagram of the forces acting on a prestressed beam with a parabolic tendon profile. Clearly, the two sets of equal and opposite transverse loads w_b *cancel* each other, and no bending stress is produced. This is reasonable to expect in the load-balancing method, since it is always the case that $T = C$, and C has to cancel T to satisfy the equilibrium requirement that $\Sigma H = 0$. As there is no bending, the beam remains straight, without having a convex shape, or camber, at the top face.

The concrete fiber stress across the depth of the section at midspan becomes

$$f_b^t = -\frac{P'}{A} = -\frac{C}{A} \tag{1.17}$$

This stress, which is constant, is due to the force $P' = P \cos \theta$. Figure 1.10 shows the superposition of stresses to yield the net stress. Note that the prestressing force in the load-balancing method has to act at the center of gravity (cgc) of the support section in simply supported beams and at the cgc of the free end in the case of a cantilever beam. This condition is necessary in order to prevent any eccentric unbalanced moments.

When the imposed load exceeds the balancing load w_b such that an additional *unbalanced* load w_{ub} is applied, a moment $M_{ub} = w_{ub}l^2/8$ results at midspan. The corresponding fiber stresses at midspan become

$$f_b^t = -\frac{P'}{A_c} \mp \frac{M_{ub}c}{I_c} \tag{1.18}$$

Equation 1.18 can be rewritten as the two equations

$$f^t = -\frac{P'}{A_c} - \frac{M_{ub}}{S^t} \tag{1.19a}$$

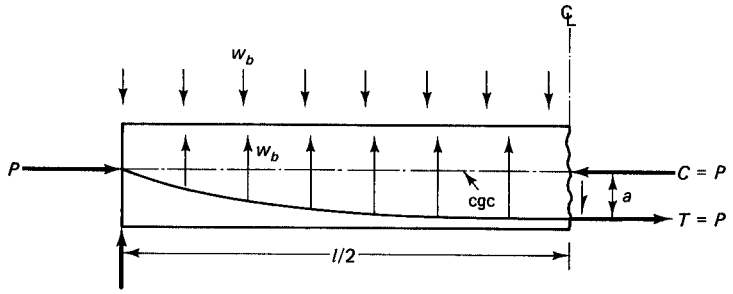

Figure 1.9 Load-balancing force on free-body diagram.

Photo 1.11 Walt Disney World Monorail, Orlando, Florida. A series of hollow precast prestressed concrete 100-foot box girders individually post-tensioned to provide six-span continuous structure. Designed by ABAM Engineers, Tacoma, Washington. (*Courtesy,* Walt Disney World Corporation.)

and

$$f_b = -\frac{P'}{A_c} + \frac{M_{ub}}{S_b} \tag{1.19b}$$

Equations 1.19 will yield the same values of fiber stresses as Equations 1.7 and 1.12. Keep in mind that P' is taken to be equal to P at the midspan section because the prestressing force is horizontal at this section, i.e., $\theta = 0$.

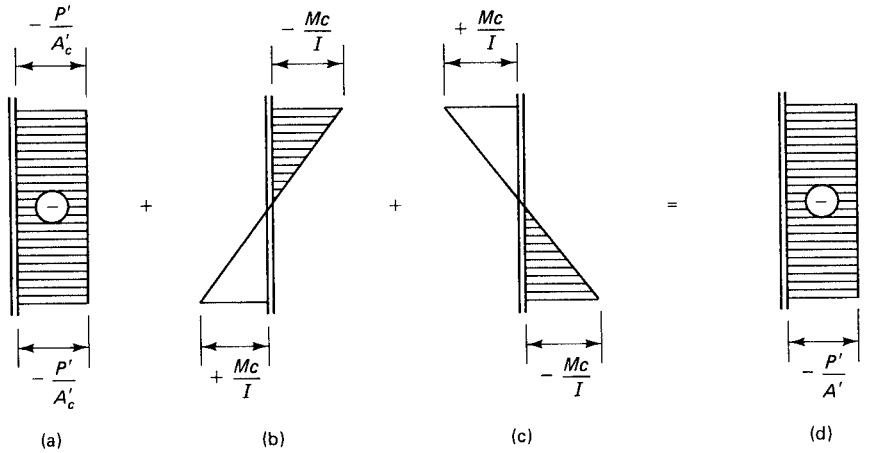

Figure 1.10 Load-balancing stresses. (a) Prestress stresses. (b) Imposed-load stresses. (c) Balanced-load stresses. (d) Net stress.

1.4 COMPUTATION OF FIBER STRESSES IN A PRESTRESSED BEAM BY THE BASIC METHOD

Example 1.1

A pretensioned simply supported 10LDT24 double T-beam without topping has a span of 64 ft (19.51 m) and the geometry shown in Figure 1.11. It is subjected to a uniform superimposed gravity dead-load intensity W_{SD} and live-load intensity W_L summing to 420 plf (6.13 kN/m). The initial prestress before losses is $f_{pi} \cong 0.70\, f_{pu} = 189{,}000$ psi (1,303 MPa), and the effective prestress after losses is f_{pe} = 150,000 psi (1,034 MPa). Compute the extreme fiber stresses at the midspan due to

(a) the initial full prestress and no external gravity load
(b) the final service load conditions when prestress losses have taken place.

Allowable stress data are as follows:

$f'_c = 6{,}000$ psi, lightweight (41.4 MPa)
$f_{pu} = 270{,}000$ psi, stress relieved (1.862 MPa) = specified tensile strength of the tendons
$f_{py} = 220{,}000$ psi (1.517 MPa) = specified yield strength of the tendons
$f_{pe} = 150{,}000$ psi (1,034 MPa)
$f_t = 12\sqrt{f'_c} = 930$ psi (6.4 MPa) = maximum allowable tensile stress in concrete
$f'_{ci} = 4{,}800$ psi (33.1 MPa) = concrete compressive strength at time of initial prestress
$f_{ci} = 0.6\, f'_{ci} = 2{,}880$ psi (19.9 MPa) = maximum allowable stress in concrete at initial prestress
$f_c = 0.45\, f'_c$ = maximum allowable compressive stress in concrete at service

Assume that ten $\frac{1}{2}$in.-dia. Seven-wire-strand (ten 12.7-mm-dia strand) tendons with a 108-D1 strand pattern are used to prestress the beam.

$$A_c = 449 \text{ in.}^2\ (2{,}915 \text{ cm}^2)$$
$$I_c = 22{,}469 \text{ in.}^4\ (935{,}347 \text{ cm}^4)$$
$$r^2 = I_c/A_c = 50.04 \text{ in.}^2$$

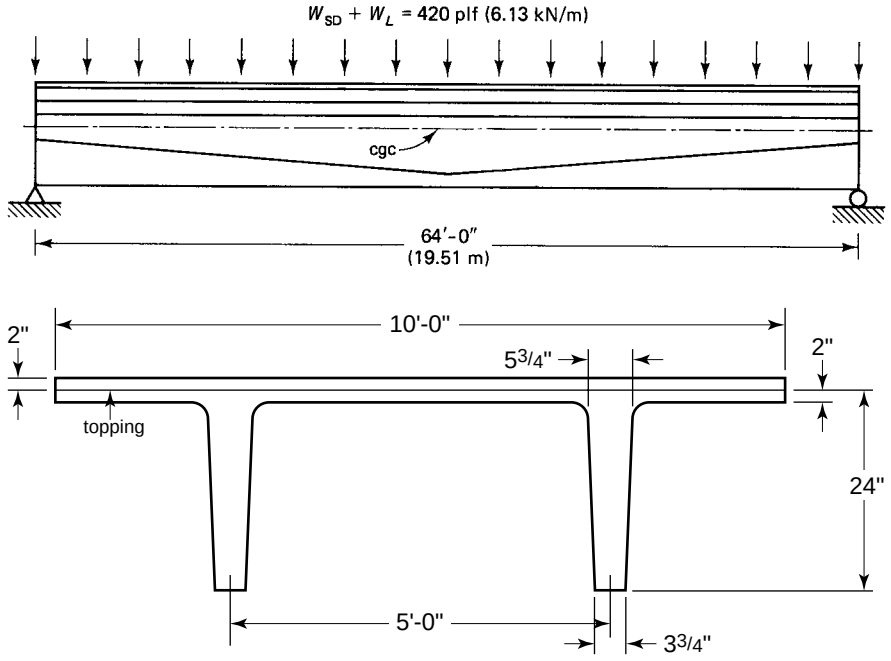

Figure 1.11 Example 1.1

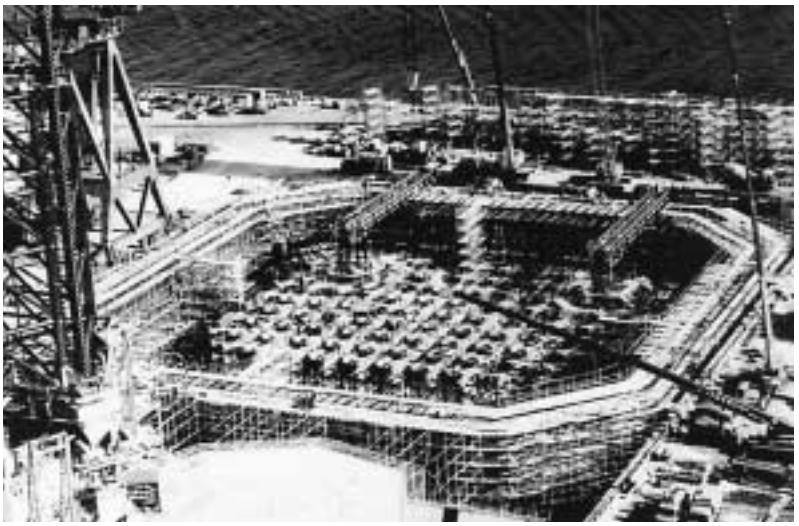

Photo 1.12 Prestressed lightweight concrete mid-body for Arctic offshore drilling platform. Global Marine Development. (*Courtesy,* the late Ben C. Gerwick.)

$$c_b = 17.77 \text{ in. (452 mm)}$$
$$c_t = 6.23 \text{ in. (158 mm)}$$
$$e_c = 14.77 \text{ in. (375 mm)}$$
$$e_e = 7.77 \text{ in. (197 mm)}$$
$$S_b = 1{,}264 \text{ in.}^3 \text{ (20,714 cm}^3\text{)}$$
$$S^t = 3{,}607 \text{ in.}^3 \text{ (59,108 cm}^3\text{)}$$
$$W_D = 359 \text{ plf (4.45 kN/m)}$$

Solution:

(i) ***Initial Conditions at Prestressing***

$$A_{ps} = 10 \times 0.153 = 1.53 \text{ in.}^2$$
$$P_i = A_{ps} f_{pi} = 1.53 \times 189{,}000 = 289{,}170 \text{ lb (1,287 kN)}$$
$$P_e = 1.53 \times 150{,}000 = 229{,}500 \text{ lb (1,020 kN)}$$

The midpan self-weight dead-load moment is

$$M_D = \frac{wl^2}{8} = \frac{359\ (64)^2}{8} \times 12 = 2{,}205{,}696 \text{ in.-lb. (249 kN-m)}$$

From Equations 1.5 and 1.7,

$$f^t = -\frac{P_i}{A_c}\left(1 - \frac{ec_t}{r^2}\right) - \frac{M_D}{S^t}$$
$$= -\frac{289{,}170}{449}\left(1 - \frac{14.77 \times 6.23}{50.04}\right) - \frac{2{,}205{,}696}{3{,}607}$$
$$= +540.3 - 611.5 \cong -70 \text{ psi } (C)$$
$$f_b = -\frac{P_i}{A_c}\left(1 + \frac{ec_b}{r^2}\right) + \frac{M_D}{S_b}$$
$$= -\frac{289{,}170}{449}\left(1 + \frac{14.77 \times 17.77}{50.04}\right) + \frac{2{,}205{,}696}{1{,}264}$$

$$= -4{,}022.1 + 1{,}745.0 \cong -2{,}277 \text{ psi } (C)$$

$$\leq f_{ci} = -2{,}880 \text{ psi allowed, O.K.}$$

(ii) ***Final Condition at Service Load*** Midspan moment due to superimposed dead and live load is

$$M_{SD} + M_L = \frac{420\,(64)^2}{8} \times 12 = 2{,}580{,}480 \text{ in.-lb}$$

$$\text{Total Moment } M_T = 2{,}205{,}696 + 2{,}580{,}480$$

$$= 4{,}786{,}176 \text{ in.-lb. (541 kN-m)}$$

$$f^t = -\frac{P_e}{A_c}\left(1 - \frac{ec_t}{r^2}\right) - \frac{M_T}{S^t}$$

$$= -\frac{229{,}500}{449}\left(1 - \frac{14.77 \times 6.23}{50.04}\right) - \frac{4{,}786{,}176}{3{,}607}$$

$$= +429 - 1{,}327 \cong -898 \text{ psi } (C) \text{ (7 MPa)}$$

$$< f_c = 0.45 \times 6{,}000 = 2{,}700 \text{ psi, O.K.}$$

$$f_b = -\frac{P_e}{A_c}\left(1 + \frac{ec_b}{r^2}\right) + \frac{M_T}{S_b}$$

$$= -\frac{229{,}500}{449}\left(1 + \frac{14.77 \times 17.77}{50.04}\right) + \frac{4{,}786{,}176}{1{,}264}$$

$$= -3{,}192 + 3{,}786 \cong +594 \text{ psi } (T) \text{ (5.2 MPa)}$$

$$< f_t = 12\sqrt{f'_c} = 930 \text{ psi, O.K.}$$

1.5 C-LINE COMPUTATION OF FIBER STRESSES

Example 1.2

Solve example 1.1 for the final service-load condition by the line-of-thrust, C-line method.

Solution:

$$P_e = 229{,}500 \text{ lb}$$

$$M_T = 4{,}786{,}176 \text{ in.-lb}$$

$$a = \frac{M_T}{P_e} = \frac{4{,}786{,}176}{229{,}500} = 20.85 \text{ in.}$$

$$e' = a - e = 20.85 - 14.77 = 6.08 \text{ in.}$$

From Equations 1.12,

$$f^t = -\frac{P_e}{A_c}\left(1 + \frac{e'c_t}{r^2}\right)$$

$$= -\frac{229{,}500}{449}\left(1 + \frac{6.08 \times 6.23}{50.04}\right) \cong -898 \text{ psi } (C)$$

$$f_b = -\frac{P_e}{A_c}\left(1 - \frac{e'c_b}{r^2}\right)$$

$$= -\frac{229{,}500}{449}\left(1 - \frac{6.08 \times 17.77}{50.04}\right) \cong +594 \text{ psi } (T)$$

Notice how the C-line method is shorter than the basic method used in Example 1.1.

Photo 1.13 Dauphin Island Bridge, Mobile County, Alabama. (*Courtesy,* Post-Tensioning Institute.)

1.6 LOAD-BALANCING COMPUTATION OF FIBER STRESSES

Example 1.3

Solve Example 1.1 for the final service load condition after losses using the load-balancing method.

Solution:

$$P' = P_e = 229{,}500 \text{ lb at midspan}$$

$$\text{At midspan, } a = e_c = 14.77'' = 1.231 \text{ ft}$$

For the balancing load, we have

$$W_b = 8\frac{Pa}{l^2} = \frac{8 \times 229{,}500 \times 1.231}{(64)^2}$$

$$= 552 \text{ plf } (8.1 \text{ kN/m})$$

Thus, if the total gravity load would have been 552 plf, only the axial load P'/A would act if the beam had a parabolically draped tendon with no eccentricity at the supports. This is because the gravity load is balanced by the tendon at the midpan. Hence,

$$\text{Total load to which the beam is subjected} = W_D + W_{SD} + W_L$$

$$= 359 + 420 = 779 \text{ plf}$$

$$\text{Unbalanced load } W_{ub} = 779 - 552 = 227 \text{ plf}$$

$$\text{Unbalanced moment } M_{ub} = \frac{W_{ub}(l)^2}{8} = \frac{227(64)^2}{8} \times 12$$

$$= 1{,}394{,}688 \text{ in.-lb}$$

From Equations 1.19,

$$f^t = -\frac{P'}{A_c} - \frac{M_{ub}}{S^t} = -\frac{229{,}500}{449} - \frac{1{,}394{,}688}{3{,}607}$$

Photo 1.14 Heidrun Offshore Oil Drilling Platform in the North Sea weighing 2.9 million Kg. It measures 110 m on each side; has four slip-form constructed hulls and module-support 50-ft. span beams (*Courtesy,* C. E. Morrison, CONOCO Inc., Houston, Texas.)

$$= -511 - 387 \cong -898 \text{ psi } (C)$$

$$f_b = -\frac{P'}{A_c} + \frac{M_{ub}}{S_b} = -\frac{229{,}500}{449} + \frac{1{,}394{,}688}{1{,}264}$$

$$= -511 + 1{,}104 \cong 594 \text{ psi } (T)$$

$$\leq f_t = 930 \text{ psi allowed, O.K.}$$

1.7 SI WORKING LOAD STRESS CONCEPTS

Example 1.4

Solve Example 1.1 using SI units

Given

Stress Data

$$f'_c = 41.4\text{MPa}$$

$$f_{pu} = 1{,}860 \text{ MPa}$$

$$f_{pi} = 0.70\, f_{pu} = 0.70 \times 1860 = 1300 \text{ MPa}$$

$$f_{py} = 1{,}520 \text{ MPa}$$

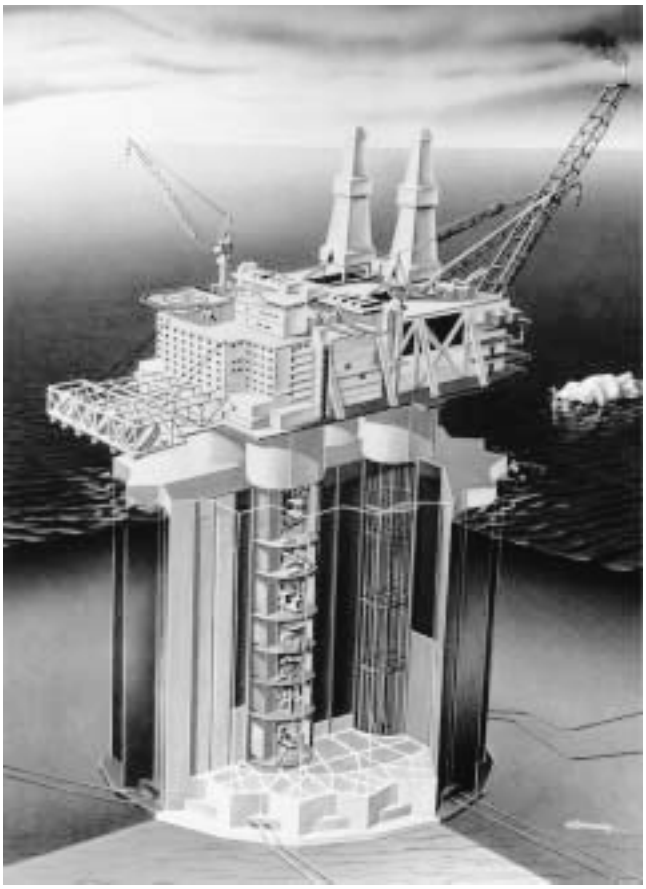

Photo 1.15 Hibernia Platform, Grand Banks, Newfoundland, 1997: 80 m water depth, 165,000 m^3, 70 MPa strength concrete and 8,000 tons of prestressing tendons; first platform designed for iceberg impacts (*Courtesy,* Dr. George C. Hoff, Mobile Research and Development Corp.)

$$f_{pe} = 1{,}034 \text{ MPa}$$

$$f_t = \sqrt{f'_c} \text{ is deflection check O.K.} = 6.4 \text{ MPa, use}$$

$$f_t = \frac{1}{2}\sqrt{f'_c} \text{ if no check made on deflection}$$

$$f'_{ci} \cong 0.8\, f'_c = 33.1 \text{ MPa}$$

$$f_{c\,i} = 0.6\, f'_{ci} = 19.9 \text{ MPa}$$

$$f_c = 0.45\, f'_c = 18.6 \text{ MPa}$$

$$A_{ps} = 10 \text{ tendons } 17.7 \text{ mm diameter} = 10 \times 99 \text{mm}^2 = 990 \text{ mm}^2$$

Section Geometry

Try 108-D1 Strand Pattern

$$A_c = 2897 \text{ cm}^2$$

$$I_c = 935{,}346 \text{ cm}^2$$

$$r^2 = I_c/A_c = 323 \text{ cm}^2$$

Photo 1.16 Pier 37 Rebuild, Seattle Washington: a 1200-ft-long by 40-ft wide pier consisting of 20-ft-long prestressed concrete deck panel supported by situ-cast concrete pile caps and prestressed concrete piles (Designed by BERGER/ABAM Engineers, Federal Way, Washington, courtesy Robert Mast, Chairman)

$$c_b = 45.1 \text{ cm} \qquad c_t = 15.8 \text{ cm}$$
$$e_c = 37.5 \text{ cm} \qquad e_e = 19.74 \text{ cm}$$
$$S^t = 59{,}108 \text{ cm}^3$$
$$S_b = 20{,}713 \text{ cm}^3$$
$$W_D = 5.24 \text{ kN/m}$$
$$W_{SD} + W_L = 6.13 \text{ kN/m}$$
$$l = 19.51 \text{ m}$$

Solution:

1. Initial conditions at prestressing

$$A_{ps} = 990 \text{ mm}^2$$
$$P_i = A_{ps} f_{pi} = 990 \times 1{,}303 = 1{,}290 \text{ kN}$$
$$P_e = A_{ps} f_{pe} = 900 \times 1034 = 1{,}024 \text{ kN}$$

Midspan self-weight dead-load moment

$$M_D = \frac{wl^2}{8} = \frac{5.24\,(19.51)^2}{8} = 249 \text{ kN-m}$$

From Equation 1.1a,

$$f^t = -\frac{P_i}{A_c}\left(1 - \frac{ec^t}{r^2}\right) - \frac{M_d}{S^t}$$

$$= -\frac{1290}{2897}\left(1 - \frac{37.5 \times 15.8}{323}\right) - \frac{249 \times 10^2 \text{ kN-cm}}{59{,}108 \text{ cm}^2}$$

$$= +0.37 - 0.42 \text{ kN/cm}^2 = -0.5 \times 10^6 \text{ N/m}^2$$

$$= 0.5 \text{ MPa } (C) < f_{ti} \text{ in tension } < f_{ci}, \text{ O.K.}$$

From Equation 1.1b,

$$f_b = -\frac{P_i}{A_c}\left(1 + \frac{ec_b}{r^2}\right) + \frac{M_D}{S_b}$$

$$= -\frac{1290}{2897}\left(1 + \frac{37.5 \times 45.1}{323}\right) + \frac{249 \times 10^2 \text{ kN-cm}}{20{,}713 \text{ cm}^2}$$

Photo 1.17 Paramount Apartments, San Francisco, CA: the first hybrid precast prestressed concrete moment-resistant 39 floor high-rise frame building in high seismicity zone, 2002. (Courtesy Charles Pankow Ltd., Design/Build contractors. Structural Engineers: Robert Englekirk Inc.; Design Architects: Elkus/Manfredi; Executive Architect: Kwan Henmi, Inc.; Owner: The Related Companies)

Photo 1.18 Rendering of the New Maumee River Bridge, Toledo. The design includes a unique single pylon clad with glass emitting LED arrays at night, single plane of stays, and a main span of 612 feet in both directions. Courtesy of the designer, FIGG Engineers of Tallahassee, Florida.

$$= -2.33 + 1.23 \text{ kN/cm}^2 = -11.0 \times 10^6 \text{ N/m}^2$$

$$= 11.0 \text{ MPa } (C) < \text{allowable } f_{ci} = 19.9 \text{ MPa, O.K.}$$

2. Final condition at service load

$$W_{SD+L} = 6.13 \text{ kN/m}$$

$$M_{SD+L} = \frac{6.13(19.51)^2}{8} = 292 \text{ kN-m}$$

Total Moment $M_T = 343 + 292 = 635$ kN – m. From Eq. 1.7a,

$$f^t = -\frac{P_e}{A_c}\left(1 - \frac{ec^t}{r^2}\right) - \frac{M_T}{S^t}$$

$$= -\frac{1024}{2897}\left(1 - \frac{37.5 \times 15.8}{323}\right) - \frac{541 \times 10^2 \text{ kN-cm}}{59{,}108 \text{ cm}^3}$$

$$= +0.29 - 0.92 \text{ kN/cm}^2 = -6.3 \times 10^6 \text{ N/m}^2$$

$$= -6.3 \text{ MPa } (C) < \text{allow } f_c = 18.6 \text{ MPa, O.K.}$$

From Equation 1.7b,

$$f_b = -\frac{P_e}{A_c}\left(1 + \frac{ec_b}{r^2}\right) + \frac{M_T}{S_b}$$

$$= -\frac{1024}{2897}\left(1 + \frac{37.5 \times 45.1}{323}\right) + \frac{541 \times 10^2 \text{ kN-cm}}{20{,}713 \text{ cm}^3}$$

$$= (-2.20 + 2.16) \times 10^7 \text{ N/m}^2 = +4.1 \times 10^6 \text{ N/m}^2$$

$$= 4.1 \text{ MPa } (T) < \text{allow. } f_t = \sqrt{f'_c} = 6.4 \text{ MPa, O.K.}$$

SELECTED REFERENCES

1.1 Freyssinet, E. *The Birth of Prestressing.* London: Public Translation, Cement and Concrete Association, 1954.

1.2 Guyon, Y. *Limit State Design of Prestressed Concrete,* vol. 1. Halsted-Wiley, New York, 1972.

1.3 Gerwick, B. C., Jr. *Construction of Prestressed Concrete Structures.* Wiley-Interscience, New York, 1993, 591 p.

1.4 Lin, T. Y., and Burns, N. H. *Design of Prestressed Concrete Structures.* 3d ed. John Wiley & Sons, New York, 1981.

1.5 Nawy, E. G. *Reinforced Concrete—A Fundamental Approach.* 6th ed., Prentice-Hall, Upper Saddle River, NJ: 2009, 936 p.

1.6 Dobell, C. "Patents and Code Relating to Prestressed Concrete." *Journal of the American Concrete Institute* 46, 1950, 713–724.

1.7 Naaman, A. E. *Prestressed Concrete Analysis and Design.* McGraw Hill, New York, 1982.

1.8 Dill, R. E. "Some Experience with Prestressed Steel in Small Concrete Units." *Journal of the American Concrete Institute* 38, 1942, 165–168.

1.9 Institution of Structural Engineers. "First Report on Prestressed Concrete." *Journal of the Institution of Structural Engineers,* September 1951.

1.10 Magnel, G. *Prestressed Concrete.* London: Cement and Concrete Association, 1948.

1.11 Abeles, P. W., and Bardhan-Roy, B. K. *Prestressed Concrete Designer's Handbook.* 3d ed. Viewpoint Publications, London, 1981.

1.12 Nawy, E. G., *Fundamentals of High Performance Concrete,* 2nd ed. John Wiley & Sons, New York, 2001, pp. 460.

1.13 Nawy, E. G., editor-in-chief, *Concrete Construction Engineering Handbook,* 2nd ed., CRC Press, Boca Raton, FL, 2008, 1560 p.

PROBLEMS

1.1 An AASHTO prestressed simply supported I-beam has a span of 34 ft (10.4 m) and is 36 in. (91.4 cm) deep. Its cross section is shown in Figure P1.1. It is subjected to a live-load intensity W_L = 3,600 plf (52.6 kN/m). Determine the required $\frac{1}{2}$-in.-dia stress-relieved seven-wire strands to resist the applied gravity load and the self-weight of the beam, assuming that the tendon eccentricity at midspan is e_c = 13.12 in. (333 mm). Maximum permissible stresses are as follows:

$$f'_c = 6{,}000 \text{ psi } (41.4 \text{ MPa})$$

$$f_c = 0.45 f'_c$$

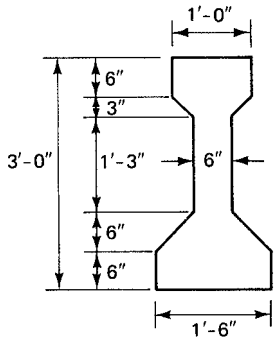

Figure P1.1

$= 2{,}700$ psi (19.7 MPa)

$f_t = 12\sqrt{f'_c} = 930$ psi (6.4 MPa)

$f_{pu} = 270{,}000$ psi (1,862 MPa)

$f_{pi} = 189{,}000$ psi (1,303 MPa)

$f_{pe} = 145{,}000$ psi (1,000 MPa)

The section properties, are:

$A_c = 369$ in^2

$I_g = 50{,}979$ in^4

$r^2 = I_c/A_c = 138$ in^2

$c_b = 15.83$ in.

$S_b = 3{,}220$ in^3

$S^t = 2{,}527$ in^3

$W_D = 384$ plf

$W_L = 3{,}600$ plf

Solve the problem by each of the following methods:

(a) Basic concept

(b) C-line

(c) Load balancing

1.2 Solve problem 1.1 for a 45 ft (13.7 m) span and a superimposed live load $W_L = 2{,}000$ plf (29.2 kN/m).

1.3 A simply supported pretensioned pretopped double T-beam for a floor has a span of 70 ft (21.3 m) and the geometrical dimensions shown in Figure P1.3. It is subjected to a gravity live-load intensity $W_L = 480$ plf (7 kN/m), and the prestressing tendon has an eccentricity at midspan of $e_c = 19.96$ in. (494 mm). Compute the concrete extreme fiber stresses in this beam at transfer and at service load, and verify whether they are within the permissible limits. Assume that all permissible stresses and materials used are the same as in example 1.1. The section properties are:

Section Properties

A_c	=	1185 in.^{2}	S_b	=	4274 in.^{3}
I_g	=	109,621 in.^{4}	S^t	=	13,128 in.^{3}
c_b	=	25.65 in.	W_D	=	1234 plf
c_t	=	8.35 in.			82 psf
			V/S	=	2.45 in.

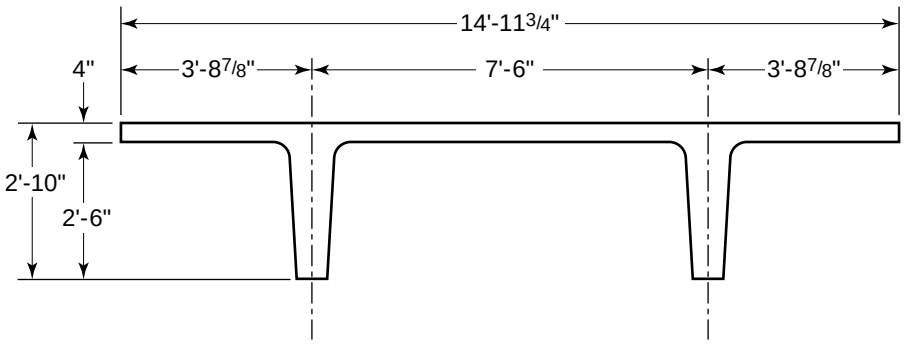

Figure P1.3

Design the prestressing steel needed using $\frac{1}{2}$-in.-dia stress-relieved seven-wire strands. Use the three methods of analysis discussed in this chapter in your solution.

1.4 A T-shaped simply supported beam has the cross section shown in Figure P1.4. It has a span of 36 ft (11 m), is loaded with a gravity live-load unit intensity $W_L = 2{,}500$ plf (36.5 kN/), and is prestressed with twelve $\frac{1}{2}$-in.-dia (twelve 12.7-mm-dia) seven-wire stress-relieved strands. Compute the concrete fiber stresses at service load by each of the following methods:

(a) Basic concept
(b) C-line
(c) Load balancing

Assume that the tendon eccentricity at midspan is $e_c = 9.6$ in. (244 mm). Then given that

$$f'_c = 5{,}000 \text{ psi } (34.5 \text{ MPa})$$

$$f_t = 12\sqrt{f'_c} = 849 \text{ psi } (5.9 \text{ MPa})$$

$$f_{\text{pe}} = 165{,}000 \text{ psi } (1{,}138 \text{ MPa})$$

the section properties are as follows:

$$A_c = 504 \text{ in}^2$$

$$I_c = 37{,}059 \text{ in.}^4$$

$$r^2 = I_c/A_c = 73.5 \text{ in.}^2$$

$$c_b = 12.43 \text{ in.}$$

$$S_b = 2{,}981 \text{ in.}^3$$

$$S^t = 2{,}109 \text{ in.}^3$$

$$W_D = 525 \text{ plf}$$

$$e_c = 9.6 \text{ in.}$$

$$A_{\text{ps}} = \text{twelve } \frac{1}{2}\text{-in.-dia, seven-wire stress-relieved strands}$$

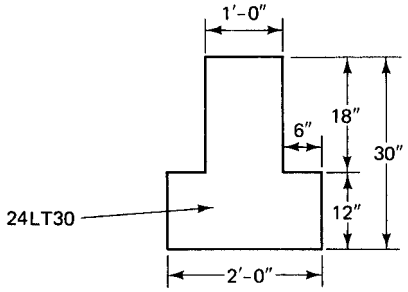

Figure P1.4

1.5 Solve problem 1.4 if $f'_c = 7{,}000$ psi (48.3 MPa) and $f_{pe} = 160{,}000$ psi (1,103 MPa).